

Creative Commons Attribution 4.0 International (CC BY 4.0)

<https://creativecommons.org/licenses/by/4.0/>

Access to this work was provided by the University of Maryland, Baltimore County (UMBC) ScholarWorks@UMBC digital repository on the Maryland Shared Open Access (MD-SOAR) platform.

**Please provide feedback**

Please support the ScholarWorks@UMBC repository by emailing [scholarworks-group@umbc.edu](mailto:scholarworks-group@umbc.edu) and telling us what having access to this work means to you and why it's important to you. Thank you.

## Article

# Simulation Study of the Applicability of the “Slice” Approach to Assessing the Water Content in Clouds from the Radar Return Signal

Boris S. Yurchak <sup>1,2,†</sup> 
<sup>1</sup> Goddard Earth Sciences and Technology Center, University of Maryland, Baltimore County, Baltimore, MD 21228, USA; bsyu33@gmail.com

<sup>2</sup> NASA Goddard Space Flight Center, Greenbelt, MD 20771, USA

† Retired Scientist.

**Abstract:** By computer simulation, the main consequences of the “slice” approach to assessing the power of a radar return signal from an atmospheric water cloud were verified. The cloud was modeled as a set of slices, which are thin layers coinciding with the wavefront of the probing radar radiation. The return signal was calculated as the convolution of the probe pulse with the cloud. The simulation was based on the previously derived “slice” radar equation, which determines the received power taking into account the statistical characteristics of fluctuations in the number of slice droplets and their water content. Estimates of the magnitude of the simulated return signal were compared with the theoretical formula for various statistical characteristics of the ensemble of droplets that make up the cloud model. The simulation result confirmed the validity of using the slice approach to interpret radar measurements of water content in clouds.

**Keywords:** radar return signal simulation; slice cloud model; slice approach



**Citation:** Yurchak, B.S. Simulation Study of the Applicability of the “Slice” Approach to Assessing the Water Content in Clouds from the Radar Return Signal. *Atmosphere* **2023**, *14*, 42. <https://doi.org/10.3390/atmos14010042>

Academic Editor: Matthew S Van Den Broeke

Received: 7 November 2022

Revised: 14 December 2022

Accepted: 21 December 2022

Published: 26 December 2022



**Copyright:** © 2022 by the author. Licensee MDPI, Basel, Switzerland. This article is an open access article distributed under the terms and conditions of the Creative Commons Attribution (CC BY) license (<https://creativecommons.org/licenses/by/4.0/>).

## 1. Introduction

Radar sounding of the atmosphere from airborne or satellite platforms is a powerful remote sensing technique for determining the microphysical properties of droplet clouds. In particular, an important task is to accurately estimate the water content of a cloud from the magnitude of the radar return signal. As a rule, the water content of clouds in radar meteorology is measured within the framework of the incoherent scattering paradigm. The measurement is based on the fact that the average power of the return signal from hydrometeors contained in the radar volume (a fictitious cylindrical volume inside the cloud at a given distance  $R$  that is bounded by the main lobe of the antenna pattern and half the spatial extent of the probe pulse) is equal to the sum of elementary return powers from these hydrometeors, e.g., [1]. Several factors can contribute to inaccuracies in the estimation of precipitation and water content of clouds by the radar method (e.g., [2]). In addition to them is a phenomenon of partially coherent backscattering due to the shape of the probing pulse, resonant or Bragg scattering and clustering scattering (e.g., [3–5]). A variation of coherence scattering is also scattering on droplets, located in a fictitious thin spherical cylinder (slice) with a radial length much smaller than the wavelength of the electromagnetic radiation of the probing radar, and a base coinciding with its wavefront [6,7]. Accounting for this phenomenon (the so-called “slice” approach) leads to the same result as the classical incoherent approach in the case of Poisson fluctuations in the number of droplets in slices contained in the radar volume. The key point of the slice approach is as follows: particles located close to the front of the incident radar radiation are considered to be at approximately the same distance from the radar, and, due to this, almost coherently reflect the incident electromagnetic wave. Therefore, the total slice’s reflectivity is the arithmetical sum of the elementary reflectivities of all the particles of the

slice due to the equality of their phases. This sum is the slice reflectivity, which determines the magnitude of the elementary return signal from a slice. The total return signal from the radar volume is the sum of the elementary return signals from the slices contained in the radar volume, taking into account their distances and, therefore, phases. The corresponded analysis, generalized in [8] for any statistical characteristics of an ensemble of particles, gives a more general estimate of the radar cross section (RCS) of a cloud compared with the previous results obtained in [6,7]. When the slice approach is applied to water droplets, the mean radar cross section ( $\langle RCS \rangle$ ) can be expressed as [8]

$$\langle RCS \rangle = \alpha^2 \langle N \rangle \langle w \rangle^2 (\xi_w^2 + \chi) \quad (1)$$

where  $\langle N \rangle = M \cdot \langle N_s \rangle$  is the mean number of droplets in the radar volume,  $\alpha = 1.13 \text{ cm/g}$  (for the C-band, i.e., the wavelength  $\lambda = 5 \text{ cm}$ ),  $M$  is the number of slices of spatial extent  $\Delta_s \ll \lambda$  each in the radar volume,  $\langle N_s \rangle$  and  $\langle w \rangle$  are the means of the number of droplets and their water content (DWC) in the slice, respectively, over the set of random realizations of droplets in the scattering volume,  $\xi_w = \frac{\text{StdDev}(w)}{\langle w \rangle}$  is the coefficient of variation (C.V.) of DWC,  $\chi = \frac{\text{Var}(N_s)}{\langle N_s \rangle}$  is the coefficient of dispersion (C.D.) of number of droplets in a slice. It is assumed that the spatial distribution of droplets in the radar volume is stationary (in the broad sense): i.e., the average number of droplets in a slice and their variance over numerous realizations are the same for all slices within the radar volume. For simplicity, the current consideration assumes that the number of slices is constant within the spatial extent of the probing pulse during the averaging period. Only small droplets of non-precipitating clouds, which are not affected by inertia effect, are considered. According to Equation (1), only for Poisson fluctuations of  $N_s$ , when  $\text{Var}(N_s) = \langle N_s \rangle$ , then  $\chi = 1$ . In this case, Equation (1) is reduced to the ordinary radar equation for incoherent scattering

$$\langle RCS \rangle = \alpha^2 \langle N \rangle \langle w^2 \rangle \quad (2)$$

Only for this particular case of Poisson fluctuations, the calculations have already been performed in previous studies [6,7]. However, the presence of this condition in the “real world” raises doubts, as noted in [9–11]. In cumulus clouds, in particular, the value  $\chi = 4.25$  was measured [9], which differs markedly from  $\chi = 1.0$  corresponding to the Poisson distribution. At high dispersion, C.D. ( $\chi$ ) is greater than 1 and  $\chi < 1$  otherwise. The slice approach enables one to obtain estimates of the magnitude of the return signal when the scattering is not incoherent and can be both larger and smaller compared with the classical case of completely incoherent scattering. Thus, further verification of the slice approach is an important task. Concurrently, experimental verification of the main provisions of any radar-cloud model is a complex organizational and technical problem (e.g., [12]). Following Equation (1), in a full-scale experiment, it is necessary to measure four microphysical parameters of a cloud in the radar sounding zone. On the other hand, computer simulation is a powerful signal analysis tool and can be applied to interpret weather radar echoes from clouds and precipitation (e.g., [13]). Thus, this study is aimed at verifying the theoretical conclusions made earlier in [8] by computer simulation of the return signal from a droplet cloud and comparing its magnitude with theoretical calculations under various conditions.

## 2. Radar Equation of Droplet Cloud for Modeling

The Equation (1) is a consequence of the representation of the variance of the slice reflectance in the form of Equation (14) from the previous article [8]

$$\text{Var}(b) = \text{Var} \left\{ \sum_{l=1}^{N_s} a_l \right\} = \text{Var}(a) \cdot \langle N_s \rangle + \langle a \rangle^2 \cdot \text{Var}(N_s) \quad (3)$$

where  $b$  is the reflectivity of a slice (slice radar equivalent length, i.e., SREL), and  $a$  is the reflectivity of a particle (particle radar equivalent length, i.e., PREL). By expressing the PREL through the DWC ( $a \propto w$ ), Equation (3) can be represented as, accurate to a constant coefficient,

$$\text{Var}(b) \propto \text{Var}\left\{\sum_{l=1}^{N_s} w_l\right\} = \text{Var}(w) \cdot \langle N_s \rangle + \langle w \rangle^2 \cdot \text{Var}(N_s) \quad (4)$$

Transforming this expression leads to Equation (1) given above. However, direct verification of Equation (1) by means of simulation is difficult. This is due to the fact that in order to obtain water content statistics of a slice, it is necessary to generate an ensemble of random water content of droplets  $\{w\}$  (i.e., PREL) for each slice and for each instantaneous random realization in the radar volume. Next, it is necessary to sum them up, average them, and calculate the variance of PRELs. The same must be done for the number of droplets in the slice. This requires significant computing resources and/or time for calculations. Therefore, a slice reflectance (SREL) characterization method was chosen by specifying a random instantaneous mean slice droplet reflectance (mean droplet water content) multiplied by a random number of droplets per slice for a given realization. Particularly, it means that the mean DWC over a slice referring to one realization (e.g.,  $k$ -th) and randomly selected one slice (e.g.,  $l$ -th) in the same realization (instantaneous mean slice water content of slice droplets, i.e., SDWC) is:

$$W_d^{(k,l)} = \frac{1}{N_s^{(k,l)}} \sum_{i=1}^{N_s^{(k,l)}} w_i^{(k,l)} \quad (5)$$

where  $N_s^{(k,l)}$  is the number of droplets in the  $l$ -th slice of  $k$ -th realization. Note that a realization is the state of the ensemble of droplets that exists in the radar volume at the moment of interaction with the probing radar pulse. Then, under the assumption that the fluctuations of  $N_s$  and SDWC are not correlated and using the known formula to express the variance of the product of two independent random variables [14], the variance of the sum of a random number of droplets with a random water content in a droplet can be represented as:

$$\begin{aligned} \text{Var}(b) &\propto \text{Var}\left\{\sum_{i=1}^{N_s} w_i\right\} = \text{Var}\left\{N_s \frac{1}{N_s} \sum_{i=1}^{N_s} w_i\right\} = \text{Var}(N_s \cdot W_d) = \\ &= \text{Var}(W_d) \cdot \text{Var}(N_s) + \langle N_s \rangle^2 \cdot \text{Var}(W_d) + \langle W_d \rangle^2 \cdot \text{Var}(N_s) \end{aligned} \quad (6)$$

In Equation (6), the indices of the realization number and the slice number are omitted owing to the assumed stationarity. Note also that  $W_d$  is the instantaneous mean water content of the slice droplets compared to  $\langle w \rangle$  which is the average water content of the slice droplets over the entire radar volume. With this representation, it is necessary to generate only one SDWC distribution function for the entire radar volume (set of slices) for one realization. The consequence of the representation in the following Equation (7) is an alternative form of the equation for the mean RCS estimation:

$$\begin{aligned} \langle \text{RCS} \rangle &= \alpha^2 M \left[ \text{Var}(W_d) \cdot \text{Var}(N_s) + \langle N_s \rangle^2 \cdot \text{Var}(W_d) + \langle W_d \rangle^2 \cdot \text{Var}(N_s) \right] = \\ &= \alpha^2 M \langle N_s \rangle^2 \langle W_d \rangle^2 [\zeta_d^2 \zeta_N^2 + \zeta_d^2 + \zeta_N^2] \end{aligned} \quad (7)$$

where  $\zeta_d = \frac{\text{Stdev}(W_d)}{\langle W_d \rangle}$  and  $\zeta_N = \frac{\text{Stdev}(N_s)}{\langle N_s \rangle}$ , which are coefficients of variation of the mean water content of a drop and the instantaneous number of droplets in a slice, respectively. The next step to apply Equation (7) for modeling is to replace the unknown mean number of droplets in the slice  $\langle N_s \rangle$  with the mean concentration of droplets in clouds  $\langle n^\circ \rangle$  of various types, known from the literature (e.g., [15]). The concentration of droplets  $n^\circ$  in the

slice can be expressed through estimates of the slice volume at a given distance  $V(R)_s$  and the mean concentration of droplets as:

$$\langle N_s \rangle = V(R)_s \langle n^\circ \rangle \quad (8)$$

In this case, the concentration  $n^\circ$  refers to the entire slice at a fixed distance, i.e.,  $n^\circ = N(R)_s / V(R)_s$ . This parameter represents the instantaneous mean (over the entire volume of the slice) concentration of the slice. The average value of this parameter over a given number of realizations is  $\langle n^\circ \rangle$ . The volume of the slice is determined by the area of the spherical surface illuminated by the main lobe of the antenna pattern at a given distance  $S(R)_s$ , and the radial size of the thin slice  $\Delta_s$ :

$$V(R)_s = S(R)_s \Delta_s \quad (9)$$

Since the  $S_s$  is proportional to the solid angle of the main lobe of the antenna pattern, we get:

$$S(R)_s = \left( 4\pi R^2 \right) \frac{\theta_{0.5}^2}{4\pi} = R^2 \theta_{0.5}^2 \quad (10)$$

where  $(4\pi R^2)$  is the area of a sphere with radius  $R$ ,  $4\pi$  is the solid angle of the entire sphere (steradian),  $\theta_{0.5}$  and  $\theta_{0.5}^2$  is the angle width and the solid angle of the main lobe of the antenna pattern at half power level (0.5), respectively. Therefore, replacing  $\langle N_s \rangle$  in Equation (7) with (8)–(10), and taking into account the number of slices in the radar volume  $M = \frac{h}{2} / \Delta_s$  ( $h = c\tau_0$  is spatial extension of the probing pulse,  $c$  is the speed of propagation of the electromagnetic radiation,  $\tau_0$  is the duration of the probing pulse), it can be represented in the form:

$$\langle RCS \rangle = \alpha^2 S^2 \Delta_s \frac{h}{2} \langle n^\circ \rangle^2 \langle W_d \rangle^2 \left[ \xi_d^2 \xi_N^2 + \xi_d^2 + \xi_N^2 \right] \quad (11)$$

Since the coefficient of variation  $\xi_N$  is also the same for the concentration, the index “ $N$ ” was left unchanged. For simulation purposes, it is more convenient to continue the consideration in terms of the power of the return signal ( $P_r$ ), which is proportional to the RCS, i.e.,  $P_r = \beta \cdot (RCS)$ , where  $\beta$  is a dimensional factor depending on the radar parameters and range. Since factors  $\alpha$ ,  $\beta$ , the slice size  $\Delta_s$  and surface area  $S$  remain unchanged in the simulation, Equation (11) can be finally written in relation to the so-called “Conditional Return Power” (CRP), which does not take into account the distance to the radar volume and the other technical characteristics of the radar (except  $h$ ):

$$\langle CRP \rangle = \frac{h}{2} \langle n^\circ \rangle^2 \langle W_d \rangle^2 \left[ \xi_d^2 \xi_N^2 + \xi_d^2 + \xi_N^2 \right] \quad (12)$$

Due to the note mentioned above, one should not concern about the CRP dimensionality being  $\text{g}^2/\text{cm}^5$ . Since  $\xi_d, \xi_N < 1$ , the bracketed expression is roughly equal to:  $[\dots] \approx \xi_d^2 + \xi_N^2$ .

### 3. Simulation Technique

#### 3.1. Return Signal Composition Algorithm

Mathematically, the return radar signal from the cloud  $U(R)$  is a convolution of the radial distribution of the slice radar equivalent length (SREL)  $Y(R)$  (adherent series of slices) [8] with a spatial extension of the probe pulse  $U_0(R)$ :

$$\dot{U}(R) = \dot{U}_0(R) \otimes Y(R) \equiv (\dot{U}_0 \otimes Y)(R) \quad (13)$$

The instantaneous SREL of an individual slice located at distance  $R$  in one realization of the return signal is equal:

$$Y(R) = \alpha N(R)_s W(R)_s = \alpha V(R)_s n^o(R)_s W(R)_s \quad (14)$$

Since the slice volume ( $V_s$ ) is practically constant within the radar volume, Equation (14) can be simplified

$$Y(R) = \gamma n^o(R)_s W(R)_s \quad (15)$$

where  $\gamma = \alpha V_s$ . The complex probe pulse is equal to:

$$\dot{U}_0(R) = \tilde{U}_0(R) \cdot \exp(-j2kR) \quad (16)$$

where  $k = 2\pi/\lambda$ , and  $\tilde{U}_0(R)$  is the rectangular envelope of the probe pulse of spatial extent  $h$ . The radar equation of the cloud should be written for the selected time delay of the return signal relative to the time of emission of the probe pulse (e.g.,  $t^*$ ) or the corresponding selected point on the range axis, e.g.,  $R^* = \frac{ct^*}{2}$ . The elementary return signals arrive at this point simultaneously from slices located within half of the spatial extent of the probing pulse [16]. Therefore, for the selected range point ( $R^*$ ), the average power of the return signal in general form is determined as follows:

$$\langle CRP(R^*) \rangle = \frac{1}{2} \left\langle \left\{ \int_0^\infty \left[ \left( \text{Re} \dot{U}_0 \otimes Y \right)(R) \right] \delta(R - R^*) dr \right\}^2 + \left\{ \int_0^\infty \left[ \left( \text{Im} \dot{U}_0 \otimes Y \right)(R) \right] \delta(R - R^*) dr \right\}^2 \right\rangle \quad (17)$$

where, the delta function  $\delta(R - R^*)$  indicates an infinitely narrow strobe function that samples the return signal value at point  $R^*$ . Theoretically, this value is the result of adding the elementary echoes from slices located within the radar volume. Using the filtering property of the delta function, Equation (17) can be represented as

$$\langle CRP(R^*) \rangle = \frac{1}{2} \left\langle \left[ \left( \text{Re} \dot{U}_0 \otimes Y \right)(R^*) \right]^2 + \left[ \left( \text{Im} \dot{U}_0 \otimes Y \right)(R^*) \right]^2 \right\rangle \quad (18)$$

Equation (18) defines the simulation algorithm for forming and sampling the return signal, which is presented in Section 4.1. It should be noted that the above consideration, as well as the simulation procedure, do not take into account the return signal distortion due to the radar receiver, which was comprehensively evaluated in [17]. It is omitted here for simplicity.

### 3.2. Simulation Parameters

#### 3.2.1. Model Distributions of Droplet Concentration and SDWC

The random concentration of drops and SDWC in a slice were modeled using a modified gamma distribution, which is represented as

$$f(x) = \frac{x^{p-1}}{\Gamma(p)} e^{-x} \quad (19)$$

where  $p = 1, 2, 3 \dots$  is the order of the distribution,  $\Gamma(p)$  is the gamma function of  $p$ , and  $x$  is the given value of the random parameter. This modification replaces  $x$  drawn from the standard gamma-function (19) with  $x + (\langle x \rangle - p)$  to make its mean a variable parameter with a fixed coefficient of variation, and vice versa. Direct use of the gamma distribution (19) is impossible since its mean and variance are the same and equal to  $p$ . Using modification, it is possible to simulate a random distribution of physical parameters with independently varied (within certain limits) mean and variance. The gamma distribution was chosen

because of its good similarity to the normal distribution. It does not have negative (non-physical) values due to the choice of appropriate values of order  $p$ . Thus, the concentration of drops in the slice and the SDWC were simulated according to the distributions:

$$f(n^\circ) = \frac{(n^\circ)^{g-1}}{\Gamma(g)} e^{-n^\circ} \quad (20)$$

and

$$f(W_d) = \frac{W_d^{q-1}}{\Gamma(q)} e^{-W_d} \quad (21)$$

where the integer parameters (orders)  $g$  and  $q$  are the variances of the concentration of drops and SDWC, respectively.

### 3.2.2. Estimation of Mean Droplet Concentration and SDWC

The mean concentration of droplets in non-precipitating clouds ranges from  $20 \text{ cm}^{-3}$  to  $500 \text{ cm}^{-3}$  [15]. Mean SDWC can be expressed thru the mean cubical radius  $\langle r_d^3 \rangle$  of the size distribution of cloud droplets:

$$\langle W_s \rangle = \frac{4}{3} \pi \rho_w \langle r_d^3 \rangle \quad (22)$$

where  $\rho_w = 1 \text{ g/cm}^3$  is the density of water. The cubical radius depends on the size distribution function  $f(r_d)$ . Following the Khragian-Mazin formula for cloud droplets [18]

$$f(r_d) = \frac{4}{r_{d,m}^3} r_d^2 \exp\left(-2 \frac{r_d}{r_{d,m}}\right) \quad (23)$$

where  $r_{d,m}$  is the mode radius, the mean cubical radius is equal to:

$$\langle r_d^3 \rangle = \left(\frac{1}{2}\right)^3 r_{d,m}^3 \frac{\Gamma(6)}{\Gamma(3)} = 7.5 r_{d,m}^3 \quad (24)$$

where  $\Gamma(x)$  is the gamma-function. In non-precipitating clouds, the mode radius ranged from 4 to  $24 \mu\text{m}$  [15]. Therefore, substituting (24) in (22) results mean SDWC ranges from 12.6 to 75.4 mg, or rounded off from 10 to 100 mg.

## 4. Theoretical and Model Estimates of <CRP>

### 4.1. Simulation Algorithm

The simulation of the return signal from the cloud was based on Equation (18) for the formation of the return signal along with the distribution functions of the random slice number of drops (Equation (20)) and SDWC (Equation (21)). The simulation procedure was performed in the Interactive Data Language (IDL) environment [19]. The simulation comprised the following stages shown in the flowchart shown in Figure 1.

1. Generating the cloud of a given length, comprising adherent train of slices, the random “reflectivity” of which is determined by a random slice number of drops and a random SDWC.
2. Generating a probing rectangular pulse with harmonic filling and a given length.
3. Forming the return signal through the convolution of the cloud’s SREL with the probing pulse.
4. Calculating the CRP corresponding to the selected point (slice, typically  $R^* = 10,000$ ) of the return signal.
5. Storing the data specified in stage 4.
6. Repeating steps 1–5 for a predetermined number of times (typically 500) to obtain a set of random realizations of the return signal.
7. Calculating the mean CRP (<CRP>) from the data stored in stage 5.



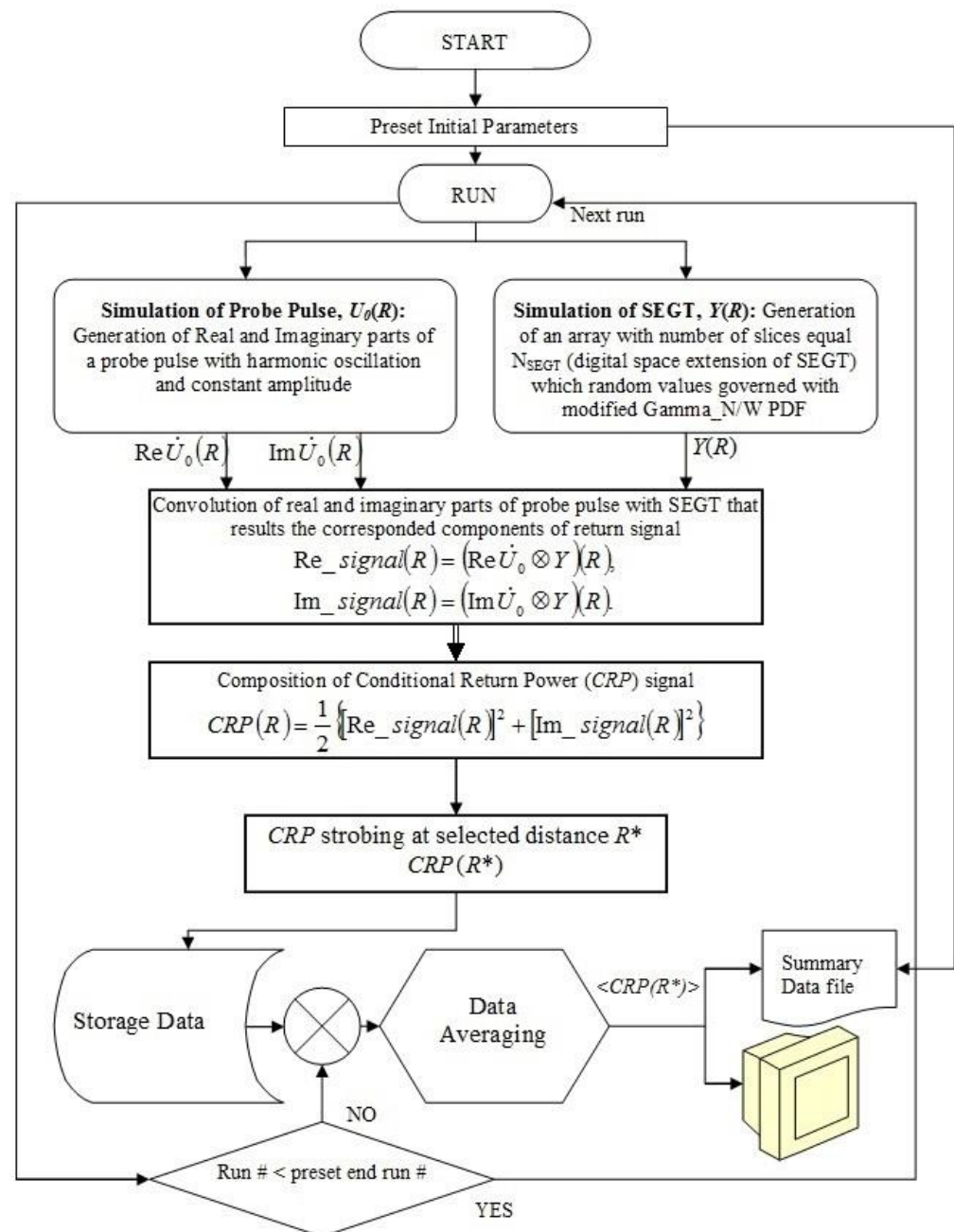


**Figure 1.** Flowchart of the simulation procedure.

#### 4.2. Comparison Characteristics

In the simulation, “measured” mean CRP was compared with the same calculated with Equation (12). This formula contains five parameters. Thus, the simulation was carried out sequentially, varying one parameter while fixing the other four. The degree of coincidence of the theoretically calculated values of the mean conditional power  $\langle CRP \rangle_F$  (according to Equation (12)) with the corresponding values of the simulated return signal  $\langle CRP \rangle_S$  was estimated using the ratio:

$$\eta(x) = \frac{\langle CRP(x) \rangle_S}{\langle CRP(x) \rangle_F} \quad (25)$$

where  $x$  is the variable parameter. The degree of coincidence between the theoretical results and the simulation results was characterized by positive (+) and negative (−) deviations



from 1 (in percent) of the average ratio for the values of the variable parameter  $x$  specified during the simulation:

$$dev^+, \% = 100 \cdot [\langle \eta \rangle + Stdev(\eta) - 1] \quad (26)$$

$$dev^-, \% = 100 \cdot [\langle \eta \rangle - Stdev(\eta) - 1] \quad (27)$$

where  $\langle \eta \rangle$  and  $Stdev(\eta)$  are the mean and standard deviation of ratio (25) for different values of  $x$ , respectively. To test the proportionality of the average CRP to the number of slices  $M$  in the radar volume, the spatial extent of the probe pulse was varied from 3000 to 12,000 slices and the spatial extent of the cloud was equal to 60,000 slices. The mean values of the concentration in the slice  $\langle n^\circ \rangle$  and SDWC  $\langle W_s \rangle$  were taken (based on the estimates in Section 3.2) in the range of 20–500  $\text{cm}^{-3}$  and 10–100 mg, respectively. The amplitude of the probe pulse was chosen as 1. The coefficients of variation  $\xi_d$  and  $\xi_N$  were set in the range from 0.05 to 0.3. The upper limit of the coefficient of variation was taken to be no greater than 0.3 due to features of the modified gamma distribution function (19). This is true for other one-mode distributions where the mean is at least three times the standard deviation to minimize negative (non-physical) parameter values.

#### 4.3. Comparison Results of Calculated and Simulated $\langle CRP \rangle$ Estimates

The simulation experiment consisted of 10 sessions. Each session consisted of several tests (5–8) for different values of the variable parameter. The comparison results are presented in Table 1. It shows the results of comparing the calculated according to Equation (12) and simulated  $\langle CRP \rangle$  estimates for various conditions. Values C.D. ( $\chi$ ) in Table 1 are not specified but obtained as a result of direct calculations based on the simulation results.

**Table 1.** Simulation conditions and results.

Session	Simulation Parameters			Simulation Results		
	Fixed	C.D. ( $\chi$ )	Variable	<CRP> Ratio: Simulated/ Calculated		Deviation from 1, %
				Avr	StDev	
1	2	3	4	5	6	7
1	$\langle n^\circ \rangle = 100; \langle W_s \rangle = 50$ $\xi_d = 0.1; \xi_N = 0.1$	1	$h = 3000, 4000,$ 6000, 8000, 10,000, 12,000	1.000	0.045	$\pm 4.5$
2	$\langle n^\circ \rangle = 100; \langle W_s \rangle = 50$ $\xi_d = 0.1; \xi_N = 0.0707$	0.5	idem	1.012	0.056	+6.8 ... −4.4
3	$\langle n^\circ \rangle = 100; \langle W_s \rangle = 50$ $\xi_d = 0.1; \xi_N = 0.2$	4.0	idem	0.987	0.025	+1.2 ... −3.8
4	$\langle n^\circ \rangle = 100; h = 6000$ $\xi_d = 0.1; \xi_N = 0.1$	1	$\langle W_d \rangle = 10, 20,$ 30, 50, 70, 100	0.983	0.040	+2.4 ... −5.7
5	$\langle W_d \rangle = 50; h = 6000$ $\xi_d = 0.1; \xi_N = 0.1$	0.2–5.0	$\langle n^\circ \rangle = 20, 50,$ 100, 200, 300, 400, 500	0.986	0.034	+2.0 ... −4.8
6	$\langle n^\circ \rangle = 100; \langle W_d \rangle = 50$ $h = 6000; \xi_d = 0.1$	0.01–9.0	$\xi_N = 0.01, 0.03,$ 0.05, 0.07, 0.1, 0.2, 0.3	1.016	0.025	+4.1 ... −0.9
7	$\langle n^\circ \rangle = 100; \langle W_d \rangle = 50$ $h = 6000; \xi_N = 0.05$	0.25	$\xi_d = 0.05, 0.1,$ 0.15, 0.2, 0.225, 0.25, 0.275, 0.3	0.986	0.060	+4.6 ... −7.4
8	$\langle n^\circ \rangle = 100; \langle W_d \rangle = 50$ $h = 6000; \xi_N = 0.1$	1	idem	1.000	0.051	+5.1 ... −5.2
9	$\langle n^\circ \rangle = 100; \langle W_d \rangle = 50$ $h = 6000; \xi_N = 0.2$	4	idem	0.995	0.058	+5.3 ... −6.3
10	$\langle n^\circ \rangle = 100; \langle W_d \rangle = 50$ $h = 6000; \xi_N = 0.3$	9	idem	0.996	0.025	+2.1 ... −2.9

As follows from Table 1, the theoretical (calculated) estimates and the “measured” values of the  $\langle CRP \rangle$  are in good agreement with each other for various combination of fixed and variable parameters. The maximum deviation range from 1 is approximately  $\pm 7\%$ . For illustration, several typical average envelopes of the return signal obtained in the 10<sup>th</sup> simulation session with  $\xi_d = 0.1$  are shown in Figure 2. As follows from this figure, after averaging over 500 realizations, the mean signal approaches a practically constant value throughout. This is a consequence of the stationarity of the simulated signal assumed in Section 2.

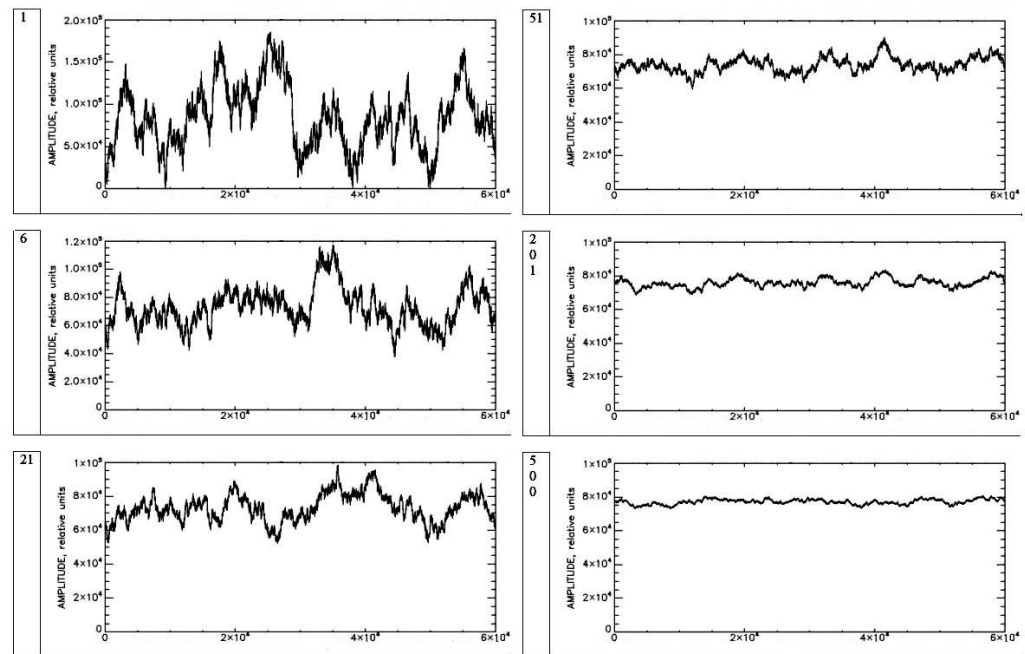


**Figure 2.** Average envelopes of the simulated return signal at  $\xi_d = 0.1$  after averaging a given number (labeled in the left column) of consecutive single realizations in session 10. The distance is indicated along the abscissa axis (in slice numbers).

Figure 3 shown below illustrates a typical simulated/calculated ratio diagram using data from session 10.

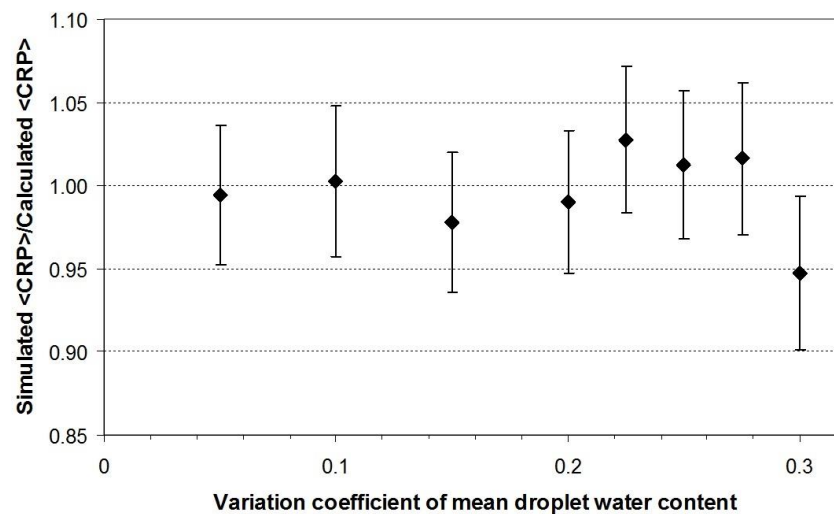


**Figure 3.** The resulting simulated/calculated  $\langle CRP \rangle$  ratios for different coefficients of variation of the mean droplet water content ( $\xi_d$ ) in session 10 (error bars indicate standard deviation).

## 5. Summary

In this study, the application of the slice approach to estimating the power of radar return signals from a water atmospheric cloud was verified using computer simulations in an Interactive Data Language (IDL) environment. The cloud simulation involved composing the random reflectivity of radially distributed adjacent slices, within which droplets scatter the radar radiation coherently. The random reflectivity of the slice was generated by combining of the random distribution of the number of slice droplets and the random distribution of mean slice drop water content (SDWC). Both distributions were specified by a modified gamma distribution. The variable statistical parameters of the cloud model are the mean values of the number of drops in the slice and SDWC, as well as their coefficients of variation. A single realization of the return signal was formed owing to the convolution of a single cloud realization with a digital model of a probing rectangular pulse of a given spatial length. The conditional return power (CRP) corresponding to the selected point (slice) of the cloud, was calculated as the sum of the squares of real and imaginary components of the elementary return signals from individual slices within the radar volume. The mean CRP ( $\langle CRP \rangle$ ) was calculated from the results of averaging the CRP over a given number of random realizations of the return signal. In this study, the number of realizations was 500, which approximately corresponds to one second of averaging for weather radars with a pulse repetition frequency of 500 Hz. The theoretical and simulation results were compared by calculating their ratio for various combinations of one variable model parameter and several fixed other. The criterion for determining the similarity of the simulation and theoretical results of the  $\langle CRP \rangle$  assessment is the deviation of the ratio from 1, expressed as a percentage. The comparison results for ten combinations of model parameters showed satisfactory agreement between the simulation and theoretical values of the  $\langle CRP \rangle$ . This result confirms the validity of using the slice approach to interpret radar measurements of water content in clouds.

**Funding:** This research received no external funding.

**Institutional Review Board Statement:** Not applicable.

**Informed Consent Statement:** Not applicable.

**Data Availability Statement:** No new data were created or analyzed in this study. Data sharing is not applicable to this article.

**Acknowledgments:** The author is pleased to express his gratitude to three anonymous reviewers of the manuscript for valuable and helpful comments.

**Conflicts of Interest:** The author declares that there is no conflict of interest.

## References

1. Atlas, D. Advances in radar meteorology. *Adv. Geophys.* **1964**, *10*, 317–479.
2. Munchak, S.J. Remote sensing of precipitation from airborne and spaceborne radar. In *Remote Sensing of Aerosols, Clouds, and Precipitation*; Islam, T., Kokhanovsky, A., Hu, Y., Wang, J., Eds.; Elsevier: Amsterdam, The Netherlands, 2018; Chapter 13; pp. 267–299.
3. Gordon, W.B. A critique of the Kerr-Siegert-Goldstein theory of radar backscatter from clouds and rain. In Proceedings of the 19th Conference on Radar Meteorology, Boston, MA, USA, 15–18 April 1980; pp. 704–707.
4. Erkelens, J.S.; Venema, V.K.C.; Russchenberg, H.W.J.; Ligthart, L.P. Coherent scattering of microwaves by particles: Evidence from clouds and smoke. *J. Atmos. Sci.* **2001**, *58*, 1091–1102. [[CrossRef](#)]
5. Lee, C.-C. Radar equation by taking into consideration the coherent scattering of radar waves from clouds and raindrops. *Sci. Sin.* **1963**, *12*, 695–708.
6. Marshall, J.S.; Hitschfeld, W. Interpretation of the fluctuating echo from randomly distributed scatterers. *Can. J. Phys.* **1953**, *31*, 962–994. [[CrossRef](#)]
7. Smith, P.L., Jr. Scattering of microwave by cloud droplets. In Proceedings of the 11th Weather Radar Conference, Boulder, CO, USA, 14–18 September 1964; pp. 201–207.
8. Yurchak, B.S. Radar volume backscatter from spatially extended geophysical targets in a “slice” approach. *IEEE Trans. Geosci. Remote Sens.* **2009**, *47*, 3690–3696. [[CrossRef](#)]
9. Kostinski, A.B.; Jameson, A.R. On the spatial distribution of cloud particles. *J. Atmos. Sci.* **2000**, *57*, 901–915. [[CrossRef](#)]

10. Kostinski, A.B.; Jameson, A.R. Fluctuation properties of precipitation: Part I. Deviations of single size drop counts from the Poisson distribution. *J. Atmos. Sci.* **1997**, *54*, 2174–2186. [[CrossRef](#)]
11. Larsen, M.L. Spatial distribution of aerosol particles: Investigation of the Poisson assumption. *J. Aeros. Sci.* **2007**, *38*, 807–822. [[CrossRef](#)]
12. Pascualucci, F.; Abshire, N.L.; Chadwick, R.B.; Kropfli, R.A. Cloud observation during the Phoenix experiment. In Proceedings of the 19th Conference on Radar Meteorology, Boston, MA, USA, 15–18 April 1980; pp. 715–717.
13. Galati, G.; Pavan, G. Computer simulation of weather radar signals. *Simul. Pract. Theory* **1995**, *3*, 17–44. [[CrossRef](#)]
14. Mood, A.M.; Graybill, F.A.; Boes, D.C. *Introduction to the Theory of Statistics*, 3rd ed.; McGraw-Hill: New York, NY, USA, 1975; p. 7.
15. Mason, B.J. *The Physics of Clouds*, 2nd ed.; Clarendon Press: Oxford, UK, 1971; p. 671.
16. Naito, K.; Atlas, D. On microwave scatter by partially coherent clouds. In Proceedings of the 12th Weather Radar Conference, Norman, OK, USA, 17–21 October 1966; pp. 7–12.
17. Doviak, R.J.; Zrnic, D.S. *Doppler Radar and Weather Observations*, 2nd ed.; Academic Press, Inc.: San Diego, CA, USA, 1993; p. 562.
18. Mazin, I.P. Microstructure of Clouds. In *Clouds and Cloudy Atmosphere*; Mazin, I.P., Khrgian, A.H., Eds.; Gidrometeoizdat: Leningrad, USSR, 1989; pp. 297–344.
19. ITT Visual Information Solution. IDL Reference Guide. Version 7.1. May 2009 Edition. ITT Visual Information Solution. Available online: <https://www.l3harrisgeospatial.com/portals/0/pdfs/idl/refguide.pdf> (accessed on 5 September 2021).

**Disclaimer/Publisher’s Note:** The statements, opinions and data contained in all publications are solely those of the individual author(s) and contributor(s) and not of MDPI and/or the editor(s). MDPI and/or the editor(s) disclaim responsibility for any injury to people or property resulting from any ideas, methods, instructions or products referred to in the content.